A new comprehensive quantitative approach for the objective identification and analysis of linear enamel hypoplasia (LEH) in worn archaeological dental assemblages

Keywords

Linear enamel hypoplasia; quantitative method; microscopic; systemic stress

Highlights

- A new comprehensive approach for assessing linear enamel hypoplasia
- Suitable for worn archaeological samples when there is an absence of visible perikymata.
- It allows for the objective identification and quantitative analysis of defect chronology and duration
- Reduces the potential for observer bias and increases the accuracy and replicability of results
- Improves the comparability of growth disruptions between studies

Abstract

We present a new comprehensive approach for the objective microscopic identification and quantitative analysis of linear enamel hypoplasia defect chronology and duration that is specifically designed for use on worn archaeological samples when there is an absence of visible perikymata. We use the anterior dentition of three individuals that were assessed for LEH using perikymata spacing and depth profiles in a previous study to demonstrate and validate the methodology. The approach draws upon two recently published methods for the identification and estimation of LEH defect chronology and combines these with new developments for objectively matching stress events across multiple teeth of the same individual. Defects on individual teeth are initially identified using the Micro Polynomial method, which relies on surface depth profiles. Defects from multiple teeth of the same individual are then used to construct a common cycle of defects that can then be more confidently attributed to episodes of systemic stress. The chronology of stress events is estimated using exponential regression equations that provide precise age estimates based on the defect distance from the CEJ. These same equations are then also used to estimate the overall duration, as well as separate stress and recovery duration for each episode. Additionally, the overall period of growth disruption that is represented by the various defects identified for each individual is also estimated. Our results indicate that the approach outlined in this paper is not only capable of replicating previous results, but that minor differences, when observed, are due to the improvement in precision and accuracy that the more objective methods employed here are able to generate. This approach not only reduces the potential for observer bias, when compared to commonly used subjective methods, but also increases the accuracy, replicability, and comparability of results while allowing for multiple aspects of LEH to be explored.

1 Introduction

Enamel hypoplastic defects are characterized by a deficiency in enamel thickness that results from episodic growth disruptions experienced during childhood (FitzGerald, 1998; Goodman & Rose, 1990; Hillson & Bond, 1997). Since enamel does not naturally remodel after deposition, these developmental defects remain as a permanent record of exposures to stress during the time of crown formation, which for the permanent anterior teeth covers a period of approximately one to six years of age (Hillson, 2014). While these defects can manifest in a variety of forms including pits, vertical grooves, and patches of missing enamel, the most commonly studied appear as horizontal grooves and are referred to as linear enamel hypoplasia (LEH) (Hillson, 1996). These linear defects follow the trend of perikymata (the surface expression of the internal incremental growth layers of enamel known as striae of Retzius) and extend around the circumference of the tooth crown (Hillson, 1996; Skinner & Goodman, 1992).

The occurrence of LEH is regularly used in bioarchaeological studies to assess the health status of past populations, to investigate adaptive life strategies, to reconstruct patterns of illness during childhood, and to generate individual life histories (Bennike, Lewis, Schutkowski, & Valentin, 2005; Gamble, Boldsen, & Hoppa, 2017; Guatelli-Steinberg, Ferrell, & Spence, 2012; King, Humphrey, & Hillson, 2005; Obertová, 2005; Palubeckaitė, Jankauskas, & Boldsen, 2002; Sandberg, Sponheimer, Lee-Thorp, & Van Gerven, 2014; Temple, 2014, 2016; Temple, Nakatsukasa, & McGroarty, 2012).

1.1 Common Methods Used

To date, there is no standardized method for the identification nor the analysis of LEH. Consequently, studies which consider LEH not only vary in the methods they employ, but also in the thresholds they use, the results they present, and how these are reported. The two most commonly used methods can be broadly separated into two categories based on the scale of the observations: macroscopic and microscopic. These differ not only in their capacity for objectivity, precision, and accuracy but also in the type of results they can yield (Cares Henriquez & Oxenham, 2017).

The first is the traditional macroscopic field method, a subjective approach whereby defects are identified as marked grooves that are visible to the naked eye or that can be felt by running a fingernail, sharp dental explorer or probe over the tooth surface (Brickley & McKingley, 2004; Buikstra & Ubelaker, 1994; Hillson, 2005). The location of defects, in relation to the cemento-enamel junction (CEJ), is recorded using standard electronic calipers. The location is then used to estimate the age at defect formation, typically using a crown developmental decile-chart by Reid and Dean (2000), and are usually reported as an age range. The severity of defects is assessed using a three grading system (1 =just discernible, 2= clear groove, 3= gross defect) (Brickley & McKingley, 2004). These studies are often limited to only discussing LEH in terms of frequency. A key issue with discussing LEH only in terms of frequencies is the assumption of uniformity between defects, which fails to recognize the range of variability in stress episode duration (Ensor & Irish, 1995). Furthermore, aside from offering no quantifiable thresholds for identifying LEH defects, macroscopic approaches are likely to under-record defects that occur in the more cervical region of the tooth crown (Hassett, 2012).

The second method, of which there are several variations, in particular with regards to the thresholds used, is a microscopic approach that identifies defects through the detection of abnormally spaced perikymata. Microscopic studies have revealed that the external manifestation of LEH defects on the tooth surface is for the most part formed as a result of variation in the spacing between perikymata rather than because they differ in terms of their form (Hillson, 2014). That is the perikymata involved in the defect depart from what is considered normal spacing for the part of the crown in which they are located. The simplest defect may involve a single wider than normal perikyma, while a larger defect may involve anywhere from 10-20+ abnormally spaced perikymata in the occlusal wall of the defect (Hillson, 2014).

Some studies that employ microscopic perikymata-based methods rely on visual identification of LEH, where defects are identified when, on visual inspection, the perikymata spacing is perceived to be deeper and/or wider in relation to adjacent perikymata (Guatelli-Steinberg, 2003; Guatelli-Steinberg et al., 2012; King, Hillson, & Humphrey, 2002; King et al., 2005; Temple, 2010; Witzel, Kierdorf, Schultz, & Kierdorf, 2008). Others, like Temple et al. (2012), use absolute values of known average perikymata spacing for the different crown thirds and identify defects when perikymata are found to be wider than the average for the region in which they manifest. Hassett (2012), on the other hand, uses a moving z-score (based on a local set of perikymata distances) to identify accentuated perikymata, and identifies defects as those that deviate significantly from the local mean perikymata spacing. Because the identification is done on a perikyma by perikyma basis, in other words, by identifying single individual perikyma that are affected, estimates of defect duration are not possible with this particular approach. Whereas, Bocaege and Hillson (2016) propose a combined visual-metric approach using LOWESS residuals.

The chronology of defects is then estimated using the Reid and Dean (2000, 2006) decile-chart or a variation thereof (e.g. Temple et al. (2012)). Stress duration is generally calculated by counting the number of perikymata found within each LEH defect or within the occlusal wall of the defect, and multiplying this by the known periodicity of perikymata formation in human populations, which range between 6-12 days, and average 8-9 days (Dean & Reid, 2001; Guatelli-Steinberg, 2008; Guatelli-Steinberg, Larsen, & Hutchinson, 2004; Reid et al., 1998; Reid & Dean, 2000; Reid & Ferrell, 2006; Smith et al., 2007).

A major limitation of this approach is the requirement of visible perikymata on the tooth surface, which excludes many archaeological samples from being suitable due to the absence of clearly visible and / or continuous perikymata along the tooth or within defects due to labial/buccal surface wear (Cares Henriquez & Oxenham, 2017; Hubbard, Guatelli-Steinberg, & Sciulli, 2009). Therefore, while there is a general consensus that microscopic methods are preferable due to their capacity to identify more instances of growth disruptions while also being able to explore the finite aspects of the defect process (Hassett, 2012; Hillson, 1992), many archaeological studies continue to employ the subjective macro method and remain limited to discussing LEH only in terms of frequency (Bennike et al., 2005; Buzon, 2006; Domett & O'Reilly, 2009; Novak et al., 2018; Obertová, 2005; Oxenham, 2006; Pechenkina, Benfer, & Zhijun, 2002; Pietrusewsky & Douglas, 2002; Shuler et al., 2012; Stodder, 1997; Temple, 2007, 2010).

A recent attempt by Cares Henriquez and Oxenham (2017) to rectify this issue prompted the development of the Micro Polynomial method. This is an alternative approach for objectively identifying LEH defects which does not rely on the presence of perikymata. Instead, this method uses microscopically constructed enamel surface depth profiles, which are fitted with a polynomial trendline, to objectively identify significant deviations in depth along the tooth surface. Currently, this approach is limited only to the identification of defects and estimates of defect duration are not possible.

Another limitation, which is often overlooked, and affects all the methods mentioned so far, relates to the matching of defects at similar chronological stages across multiple teeth of the same individual. While this is not done by all studies, it provides a means of discounting defects that might have resulted from traumatic injury, congenital disorders, or data noise (Bennike et al., 2005; Cares Henriquez & Oxenham, 2017; Hillson, 1996, 2014; King et al., 2002). Those studies which undertake this matching differentiate between unmatched defects and those that have been matched chronologically on more than one tooth, with only the latter being attributed to systemic stress. It is not uncommon for the estimated chronology of the defects that represent the same episode of stress to vary slightly from one tooth to another. Reid and Dean (2000) suggest that the average age, comprised of the individual estimates of all teeth in the same individual, is likely to provide the best overall estimate of the true chronological age at the time of illness. Hence, the matching process requires the researcher to arbitrarily decide which defect on one tooth is most likely to match another similarly aged defect on another tooth and thus represent the same episode of stress. This need for individual observer judgment increases the potential for observer bias and can significantly affect the replicability and accuracy of results.

As noted by a number of researchers, (e.g. Bocaege and Hillson (2016); Goodman and Armelagos (1985); Hindle (1998); Lukacs (1989)) the standardization of LEH defect identification and analysis is crucial for addressing what Bocaege and Hillson (2016, p. 749) see as “the current substantial bias in the bioarchaeological assessment of health in the past”. Lukacs (1989, p. 264) stresses that in order for comparative studies to produce accurate and meaningful conclusions “results that are not reproducible and high levels of inter-observer error cannot be tolerated” and suggests that “imprecision can be avoided only if investigators carefully specify the methods used in their research."

1.2 Solution

This study presents a comprehensive microscopic approach not only for the objective identification but also for the objective and quantitative analysis of LEH defects that is designed explicitly for archaeological samples that cannot make use of perikymata-based methods due to the absence of visible and / or continuous perikymata.

It draws upon two recently published objective methods for the identification and chronology estimation of LEH defects by Cares Henriquez and Oxenham (2017, 2018) and combines these with new developments which include an objective method for 'matching' defects across multiple teeth of the same individual, as well as for estimating the duration of stress episodes. Also, this study makes several recommendations to work towards the standardization of reporting of results. This paper aims to present a comprehensive approach that can be used to examine archaeological samples which reduces the potential for observer bias and increases the accuracy and replicability of results to ensure the comparability of growth disruptions between studies.

2 Materials and Method

The comprehensive approach presented in this paper follows a workflow that is comprised of a series of steps, each of which is described in detail below and summarised in Figure 1. A number of the steps outlined rely on spreadsheet software and make use of Microsoft Excel. However, the choice of spreadsheet program is left to the researcher, with a number of proprietary and non-proprietary alternatives being available.

2.1 Sample

The individuals used in this study were all sampled from archaeological sites located in northern Vietnam. These include two individuals from Con Co Ngua, a pre-Neolithic site dated to the early 7th millennium BP, and one individual from Nui Nap, a Metal period assemblage dated to 1700 BP (see Oxenham (2016); Oxenham et al. (2018)) . The dental sample was comprised of seven anterior maxillary teeth with overlapping development schedules from individuals 77NNM 18KB (Nui Nap), 80CCNM 11a and 80CCNM 47a (Con Co Ngua), which were used in a previous study by Cares Henriquez and Oxenham (2017) to illustrate a preliminary exploration of the approach being presented in this paper. These samples were originally selected due to having little to no occlusal wear (more than 90% of its original crown height was present), having no concretion obscuring the surfaces, having more than one anterior tooth present for the individual, and more importantly, for having minimal labial/buccal wear resulting in the presence of visible, albeit not always continuous, perikymata. The analysis of these samples was undertaken using epoxy replicas that were produced as part of the earlier study mentioned above.

2.2 Microscopic Analysis: Enamel Surface Depth Profiles

Enamel surface depth profiles for each tooth were constructed by collecting data along the vertical axis of each tooth crown (y-axis), from the CEJ to the incisal edge, using a Sensofar Plu Neox confocal microscope. When positioning each tooth prior to scanning, care was taken that the central vertical axis of each tooth was aligned with the y-axis of the microscope. A permanent pen was used to mark the point along the CEJ where the transect would be recorded to assist with the reproducibility of results should re-scanning of the sample be required at a later date. Additionally, care was also taken to ensure that the cervical and incisal ends of the tooth were level with each other along the z-axis so that the varying depths along the tooth surface from the objective were evenly distributed and remained within the upper and lower limits of the microscope's z-axis. Although only a single transect of data is required to identify defects, a 2 x ~27 grid area (1.180 x 11.07 mm) topography scan was carried out for each tooth using the settings listed in Table 1. The topography scans were then used to select the ideal locations on which to then record three data transects, i.e., surface profiles). This ensured that areas on the tooth surface with obvious abnormalities that have the potential to interfere with the results could be avoided (i.e., depressions associated with cracks, pits, or elevations associated with concretion or other materials adhered to the enamel surface). Furthermore, multiple transects allowed for visual comparison and confirmation that the data were in fact representative of the surface being examined, and, that they were not affected by noise associated with focusing errors, which can occur from time to time.

Table 1. Sensofar Extended Topography Scan Settings

Sensofar Settings	
Operation Mode: Default	Continuous autofocus
Measurement: Extended	Smart
Topography	Large and small range
Objective: EPI 20X-N (1-micron	2x speed
steps)	Threshold: 1
Confocal Z-scan: 200.0 microns	y and z resolution: 1.6 µm
Resolution: 2	
Overlapping Area: 15 (minimum of	
10)	

2.3 Objective identification of LEH defects: Polynomial, Negative Residuals, and Moving Standard deviation

Identification of LEH defects was carried out using the Micro Polynomial method, as published in Cares Henriquez and Oxenham (2017), with minor adjustments. This method used enamel surface depth profiles of teeth to capture changes in depth (i.e., depressions), which can be used as evidence of LEH. The higher resolution and automated functionalities of the confocal microscope used in this study eliminated the need to employ additional criteria that were recommended to decrease the chance of data error associated with manual focusing (see Cares Henriquez and Oxenham (2017)).

Each enamel surface profile was fitted with a sixth order polynomial trendline, which was then used to calculate negative residuals and identify depressions along the enamel surface using Microsoft Excel. Areas along the tooth surface where residuals deviated by more than one centred moving standard deviation from the fitted sixth order polynomial were accepted as possible evidence of systemic stress. Here, a moving standard deviation rather than simple standard deviation is required to deal with effects that the underlying perikymata spacing is expected to have on the morphology of LEH defects, especially at the cervical and incisal ends (Cares Henriquez & Oxenham, 2017).

The centred moving standard deviation was calculated as

$$\sigma = \sqrt{\frac{\sum(x_i - \mu)^2}{N}}$$

where x_i represents an observation of point i (each observation is the residual or difference between an observed data point along the tooth surface and the fitted polynomial), μ is the mean of observations within the moving sample (i.e. it is the average of the residuals across the quarter of observations centred on the focal point, so that it is comprised of an eighth of the total observations before and after the focal point), and N represents 1/4 of the total sample size. The exact number of observations or data points to be included is dependent on the individual crown height and so will vary from tooth to tooth.

Using too few observations for N may result in the distribution being too volatile (i.e., follows the actual dataset too closely) making it difficult to appreciate the underlying pattern, while using a higher number of observations can lead to a dataset that is too smooth, thus missing some of the changes occurring on a smaller scale. While there is a certain amount of freedom in deciding exactly how many observations should be included (based on the resolution at which the data is captured), the maximum number of observations should not exceed 1/3 of the total sample size. The reason being that, again, this value corresponds to the varying geometric orientation of Striae of Retzius that can be observed along the tooth crown (with the largest variation occurring between the different tooth thirds), and so is used to deal with the effects that these have on the prominence and depth of LEH defects (Cares Henriquez & Oxenham, 2017; Guatelli-Steinberg, 2008; Hillson & Bond, 1997). It should also be noted that this method of averaging the standard deviation cannot be applied in the same way to the first and last eighth of the data, because the range would exceed the end-points of the data set. This is a common problem in moving averages and requires a simplifying assumption as the average approaches the end-point.

In this case, due to the higher resolution of the data collected with the confocal microscope, ~6000 vs 200 data points when compared to that collected using a custom-built measuring microscope in the approach taken by Cares Henriquez and Oxenham (2017), the number of observations included in the centred moving standard deviation was decreased from one third to one quarter. This reduction in the number of observations included in the calculation has a two-fold effect: 1) it can better capture the gradual changes in enamel depth that occurs across the tooth crown; 2) it reduces the number of data points at the beginning and end of the tooth for which no values can be assigned.

Additionally, in assigning standard deviation values to the first and final $1/8^{th}$ of the dataset, each end was treated slightly differently. This was to deal with focusing issues that are most likely to occur at the incisal edge, as well as possible artificial defects resulting from underfitting of the polynomial, which can occur on both ends of the dataset, while still taking into account the effects that the underlying spacing of perikymata have on the morphology of defects. Therefore, on the incisal end, the first 1/8 of the moving standard deviation is equivalent to the standard deviation of the entire tooth. While on the cervical end, the last 1/8 of the moving standard deviation is equivalent to the value of the last viable data point in the residual series for which the centred moving standard deviation could be calculated.

This study considered the start of each defect (i.e. each depression that has been identified as falling below the 1 standard moving deviation) as commencing at the last previous negative residual data point to fall at 0, while the end of a defect as terminating at the subsequent negative residual data point that reaches back up to 0.

2.4 Estimates of Crown Height Wear

In the absence of a more objective method for estimating the amount of wear-induced reduction of dental crown height on the anterior dentition, the following practical standard for crown height wear estimates was employed:

0% =	mamelons still visible on some part of the incisal edge
5% =	mamelons not visible, no dentin visible
10% =	≤ 1mm thickness of dentin visible (observed as a linear strip of wear in a labial to lingual direction)
>10% =	> 1mm of dentin visible. crown height estimated based on average height of unworn tooth for population

2.5 Defect Chronology

Defect chronology estimates, that is, the age of the individual at the time of defect formation, were calculated using recently published distance-based exponential regression equations by Cares Henriquez and Oxenham (2018). Using these equations, which are based on previously published histologically derived data by Reid and Dean (2000, 2006), the defect location, in other words, the distance of the start of the defect from the CEJ (in mm), is used to calculate the defect chronology. These equations are based on a decile system, where the *y*-intercept (or the maximum age of a defect) is equivalent to the maximum age of crown completion (the

10th decile) for the specific tooth type that is being examined. Therefore, in practice, the distance of the defect from the CEJ must also be standardized before inserting into the equations. In the equations, "x" is the distance of the defect from the CEJ along a standardized 10mm tooth. Standardizing allows direct comparison with the decile methods because each millimetre represents a decile. The standardized x for each defect was calculated as:

$$x = \left({}^{d}\Big/_{\frac{l}{1-m}} \right) \times 10$$

where (d), the observed distance of the start of the defect from the CEJ in mm, is divided by the length of the tooth available (i.e. length of the surface profile) in mm (l), which itself is divided by the percentage of tooth that is missing ($1 - m$). This is then multiplied by ten to give the distance on a standardized 10mm tooth.

It should be noted that, currently, unless examining the presence of LEH defects histologically, more often than not, certain assumptions are required when estimating the chronology and stress duration of LEH defects. This is due to needing to rely on estimates for initiation of tooth mineralization, cuspal enamel formation times, as well as periodicities that are derived from populations other than of the subject sample in order to perform the calculations. These variables have not only been shown to vary between different populations, but also from one individual to the next. This study relies on equations that use enamel growth developmental schedules derived from a Northern European sample. The specific equations used to calculate the chronology of defects for the sample in this study are listed in Table 2 and are specific to the tooth type being examined. (FitzGerald, 1998; Goodman & Song, 1999; Reid & Dean, 2000, 2006; Reid & Ferrell, 2006; Smith, 2008; Smith et al., 2010).

The estimated chronology (in years) for defects on individual teeth are presented in the results section (see Table 4).

Table 2. Equations for LEH Defect Chronology (from Cares Henriquez and Oxenham (2018)).

Tooth Type	Equation
Upper central incisor	$\text{Age}^{a} = 5e^{-0.146x}$
Upper lateral incisor	$\text{Age} = 5.1e^{-0.106x}$
Upper canine	$\text{Age} = 5.3e^{-0.112x}$

[a] Age in years (multiply by 365 for age in days).

There are two main practical applications for these equations. The first is to use the equations to convert each defect's distance from the CEJ to time. This can be done manually by inputting the standardized distance into the equation or using the LEH Chronology Calculator, a Microsoft Excel tool released earlier this year, which standardizes and converts the defect location from a distance to time (Cares Henriquez, 2019). The second is simply to convert all the continuous negative residual data from a scale of distance to time using the equations and a spreadsheet program such as Microsoft Excel.

2.6 Defect Duration

Stress duration for each defect was estimated by utilizing the same exponential regression equations by Cares Henriquez and Oxenham (2018) that were used to estimate defect chronology (see Table 2 for equations). This was done by converting the standardized defect start and end locations (distance from CEJ in mm) to time (years) and then subtracting the start age from the end age to compute the overall defect duration.

Microscopic analysis has shown that LEH defects are comprised of two main phases. The first is a period of stress where growth is disrupted and can be observed in the occlusal wall of the defect. This phase is followed by a period of recovery, which can be observed in the cervical wall of the defect (Guatelli-Steinberg, 2008; Hillson, 2014; Hillson & Bond, 1997). The estimated overall defect durations for individual teeth (stress + recovery) are reported as days in Table 4. It should be noted that in this paper we differentiate between 'defect duration' and 'episode duration', with the first referring to the overall duration of a defect that has been observed on an individual tooth, while the latter refers to a defect that has been matched on multiple teeth of the same individual.

2.7 Common Cycle of Defects: Multiple Teeth of the Same Individual

A modified approach was used for assessing LEH when multiple teeth of the same individual were available. This involved objectively identifying a cycle of defect patterns that were common across multiple teeth of the same individual and then using these to estimate the chronology and duration of LEH defects.

First, the residuals, which were calculated for each tooth by fitting a sixth order polynomial to the enamel surface profile, were converted to time using the exponential regression equations by Cares Henriquez and Oxenham (2018). Excel formulas were used to apply the appropriate regression equation to each data series, as well as to standardize each *x* data point (see 2.4 Defect Chronology) (distance value) and incorporate any estimates of crown height wear. An example Excel formula for converting negative residuals from distance to time, including standardization of *x* data points and crown wear estimates is given in Table 3.

Table 3. Example of Excel formula for transforming negative residuals from distance to time on data from central incisor

Central Incisor Age Equation (northern European)	$5e^{-0.146x}$
Wear	12%
Defect distance from CEJ*	3.5mm
Total tooth height	10.97mm
Excel Formula	=(5*EXP((3.5/(10.97/(1-12/100))*(10))*-0.146))

* *(not standardised)*

The converted residual data of the multiple teeth being examined were then aligned with each other according to time. This was achieved using Excel INDEX and MATCH functions so that each series commenced at the oldest age of crown completion that fell within the developmental schedule of all teeth being examined. When examining multiple teeth, the time frame available for identifying and matching defects was limited by the oldest age of cuspal completion and the youngest age of crown completion across the specific teeth being examined.

Next, Solver, a Microsoft Excel add-in program was used to offset each series of negative residuals by up to +/- 200 days. The choice of this upper and lower limit is left to the analyst. However, here it was set to approximately six months, which is equivalent to the average maximum number of days of enamel growth represented by a single decile in the anterior dentition (based on data by Reid and Dean (2000) used for estimating defect chronology in section 2.5). Solver can be used for What-If Analysis to find an optimal maximum or minimum value for a formula in one cell (referred to as the objective cell), which is subject to constraints or limits, on the values of other formula cells. In this case, Solver was used to solve the precise number of days that each individual series of residuals needed to be offset from each other (shifting either forward or backward) in order to produce the greatest number of instances where all three residual values (one from each tooth) fell below one negative standard deviation that was calculated for each series. That is to say, where there is the most overlap between the pattern of common defects across the multiple teeth.

In order to better illustrate what this process achieves three identical hypothetical series of negative residuals were used, each converted to time based on a different tooth class, to construct a common cycle and demonstrate how Solver is used to do this (see figures 3, and 4 and 5 in the Results section). A common cycle of defects was then constructed from the offset data series by calculating an average residual series. This common cycle of defects (see Figure 5) was then fitted with the average moving standard deviation of all teeth being examined and used to identify the start and end points of each common defect.

A common cycle of defects was then constructed for all three individuals examined in this study following the above process, the results of which can be seen in Table 5, and then used for estimating defect chronology and defect durations.

Defect chronology and defect durations were calculated in the same way as when examining individual teeth (see sections 2.4 and 2.5). The start of the defect location was converted to time using the Cares Henriquez and Oxenham (2018) exponential regression equations to produce defect chronology, and overall episode duration estimates were calculated by subtracting the start time from the end time. In addition, the overall episode duration, stress duration and recovery duration estimates were calculated separately for each episode identified within the common cycle of defects of each individual. For this purpose, the end of stress and beginning of recovery was judged as being the lowest negative residual point within the observed defect after which no further significant decline can be observed.

2.8 Individual Growth Disruption Estimates

The total growth disruption for the individual was calculated by summing up all of the overall episode durations (stress + recovery) from the constructed common cycle of defects and are presented in Table 5.

Figure 1 Flowchart of comprehensive approach for the identification and analysis of LEH as presented in this paper.

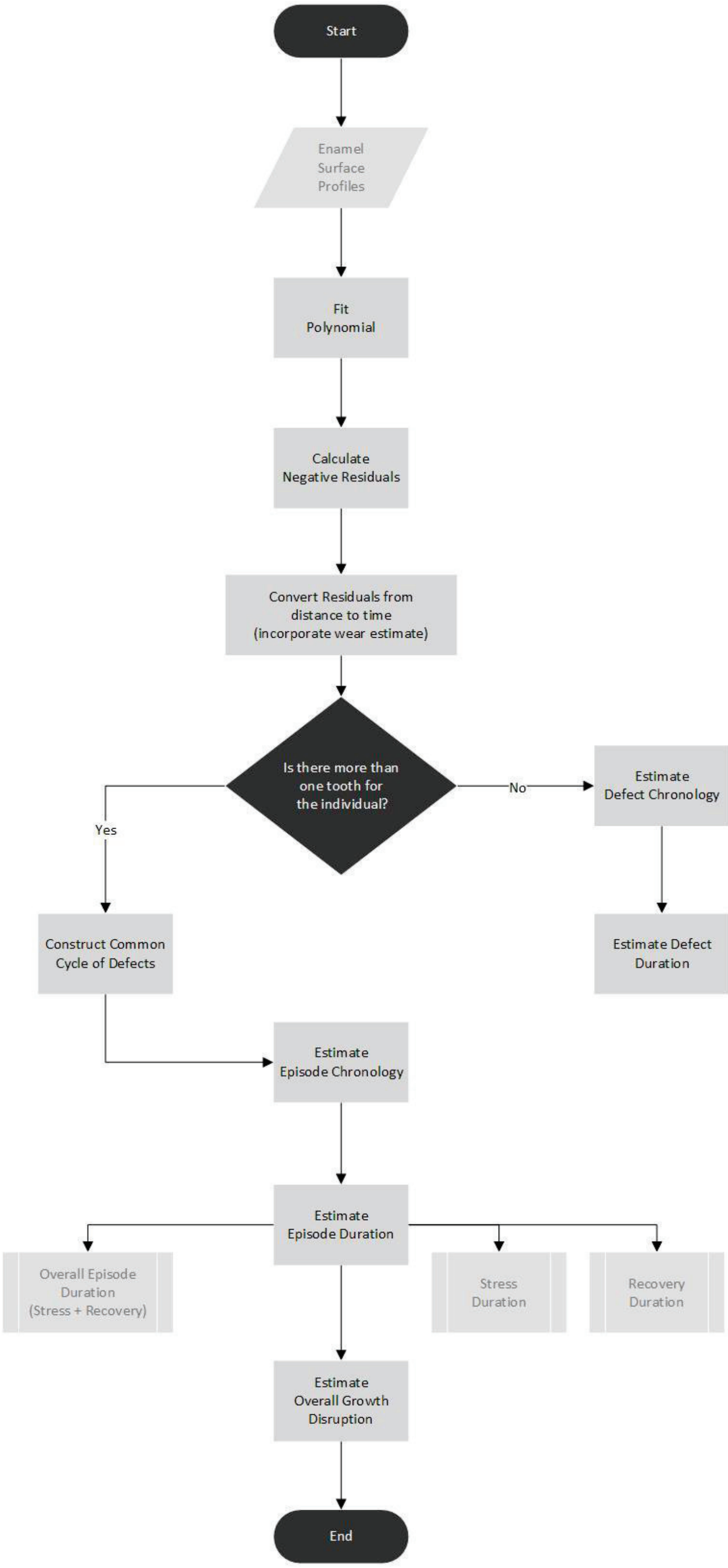
Start
Enamel Surface Profiles
Fit Polynomial
Calculate Negative Residuals
Convert Residuals from distance to time (incorporate wear estimate)
Is there more than one tooth for the individual?
Yes
No
Estimate Defect Chronology
Estimate Defect Duration
Construct Common Cycle of Defects
Estimate Episode Chronology
Estimate Episode Duration
Overall Episode Duration (Stress + Recovery)
Stress Duration
Recovery Duration
Estimate Overall Growth Disruption
End

3 Results

3.1 Microscopic analysis and Micro Polynomial Identification

The upper left central incisor (tooth 21) of individual CCNM47a is used here to illustrate the different steps in the method presented in this paper for the identification and analysis of LEH defects using individual teeth (tooth number is given in parenthesis and follows FDI World Dental Federation notation style). Figure 2 shows the rotated enamel surface profiles for CCNM47a (tooth 21), which has been fitted with a sixth order polynomial trendline (seen as a dashed line). While the data has been rotated to visualize the tooth surfaces, all calculations are performed on the original non-rotated data.

Figure 2 Enamel Surface CCNM47a 21

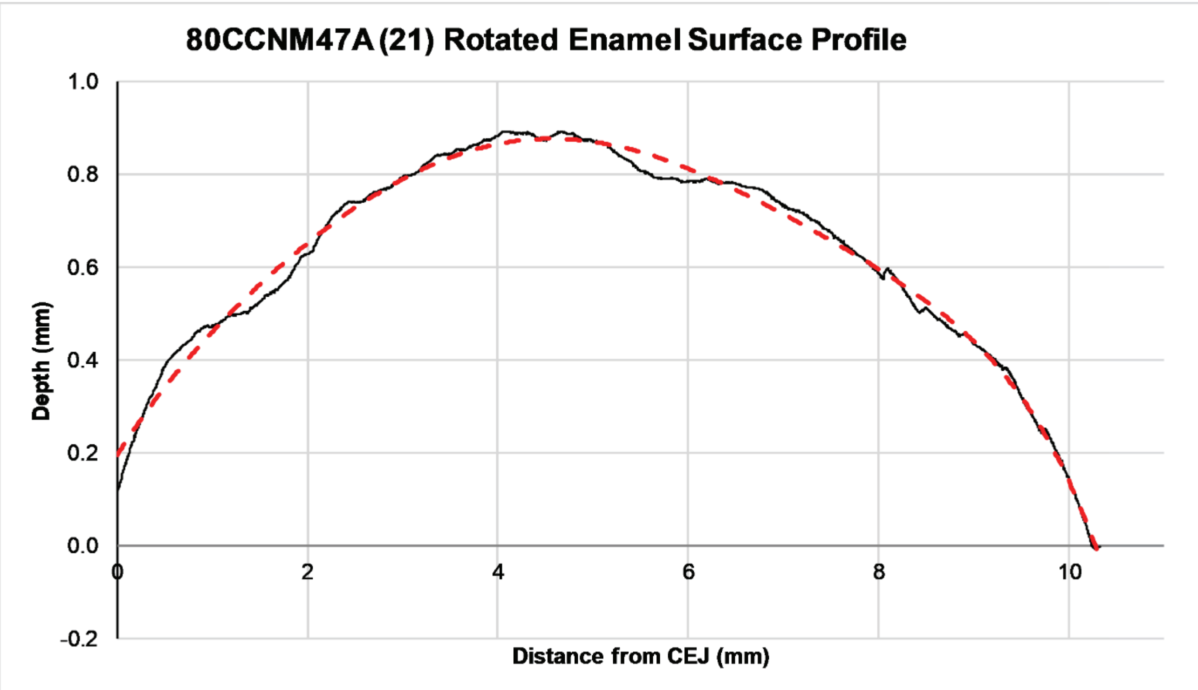

Figure 3 shows the negative residuals series converted from distance (mm) to time (days) for the upper left central incisor of individual 80CNNM47a (tooth 21) as a solid line. The dashed line represents the centred moving standard deviation, which is used to objectively identify depressions along the enamel surface that deviate by more than one standard deviation from the fitted sixth order polynomial. Five such instances were observed on the upper left central incisor (tooth 21) of 80CNNM47a, which can be visualized in Figure 3 and are summarised in Table 4. The first defect began at 516 days (1.4 years) and had an overall defect duration of 56 days. Defect two occurred at 584 days (1.6 years), with an overall defect duration of 14 days. Defect three was observed at 744 days (2.0 years) and had a total defect duration of 140 days. The fourth defect was observed at 1345 days (3.7 years), with an overall defect duration of 212 days. While the fifth and final defect occurred at 1759 days (4.8 years) with a total defect duration of 66 days.

Figure 3 Negative Residuals and Moving Standard Deviation for 80CNNM47a (21)

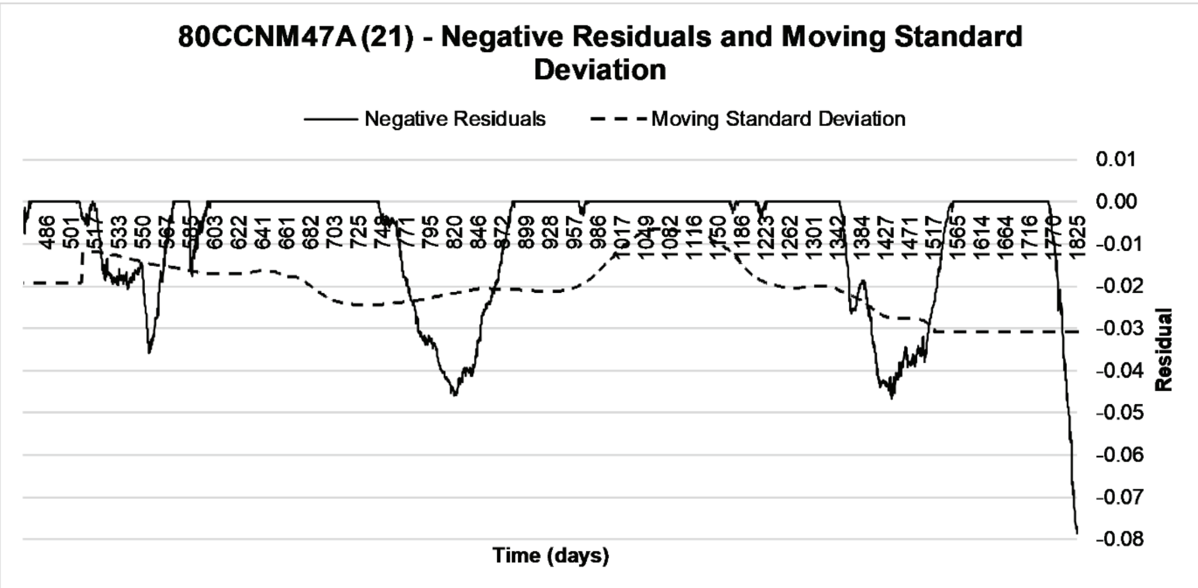

3.2 Stress Chronology and Stress Duration (Individual Teeth)

Table 4 presents the stress chronology and stress duration results of all identified defects on the dentition of 80CNNM47a, as well as the other two individuals being examined in this paper, 77NNM18KB and 80CCNM11a. Included in this table, are each identified defect's original location (distance from CEJ), chronology and overall defect duration (stress + recovery). Also, for each tooth that was examined, the overall observed tooth height and percentage of estimated crown height wear are also given.

A total of 11 defects were identified across three upper maxillary teeth of individual 77NNM18kb using the Micro Polynomial method. Of these, four defects were observed on the upper right central incisor (tooth 11), three defects on the upper left lateral incisor (tooth 22), and four defects on the upper right canine (tooth 23). The chronology of defects ranged from 1.3 to 4.5 years of age. Overall defect duration, that is, stress + recovery time ranged from 45 to 227 days. No matching was undertaken when examining individual teeth (see section 3.3 for objective matching of defects).

For individual 80CCNM11a, the Micro Polynomial method identified a total of nine defects across the two teeth examined. The upper left central and lateral incisors (teeth 11 and 12) were both estimated to have approximately 10% wear, with three defects identified on each tooth. The chronology of defects ranged from 1.4 to 4.8 years of age while the overall defect duration was found to range between 51 to 230 days.

For individual 80CCNM47a, a total of twelve defects were found across the two teeth examined. Five defects were identified on the upper left central incisor (tooth 21), and seven defects on the upper left lateral incisor (tooth 22). The chronology of defects ranged from 1.4 to 4.8 years of age. Overall defect duration ranged from 14 to 212 days.

Table 4. Individual Tooth Defects as well as Chronology and Duration as Identified using MPM

ID	Tooth	Tooth Height	CH Wear* %	Defect No.	Start (mm)	End (mm)	Chronology (years)	Defect Start (d)	Defect End (d)	Defect Duration (d)
77NN M18kb	11	9.60	0	1	8.63	9.26	1.3	491	447	45
				2	5.58	7.16	2.1	781	614	167
				3	2.58	3.88	3.4	1239	1012	227
				4	0.90	1.55	4.4	1592	1443	150
	22	7.51	0	1	4.73	5.81	2.2	820	955	136
				2	2.08	3.34	3.2	1162	1389	226
				3	0.21	0.95	4.5	1627	1807	180
	23	9.25	0	1	7.91	8.71	1.8	674	743	68
				2	5.44	6.56	2.4	874	1001	126
				3	3.78	4.50	3.1	1122	1224	102
				4	1.21	2.25	4.0	1473	1672	199
80CCN M11a	11	10.61	10	1	8.87	10.21	1.4	516	608	93
				2	5.22	7.44	2.0	726	956	230
				3	3.17	3.92	3.1	1123	1232	109
				4	1.07	2.13	3.8	1401	1598	197
				5	0.00	0.29	4.8	1761	1825	64
	12	8.64	10	1	7.82	8.40	2.0	734	785	51
				2	4.60	5.68	2.7	995	1120	126
				3	2.46	3.55	3.4	1258	1418	160
				4	0.93	1.61	4.3	1558	1679	120
80CCN M47a	21	10.33	0	1	8.21	8.94	1.4	516	572	56
				2	7.90	8.06	1.6	584	597	14
				3	5.13	6.35	2.0	744	884	140
				4	1.12	2.16	3.7	1345	1557	212
				5	0.00	0.26	4.8	1759	1825	66
	22	9.18	0	1	8.34	8.71	1.9	681	711	30
				2	6.60	7.18	2.2	813	870	57
				3	5.62	6.38	2.4	891	973	82
				4	3.14	4.40	3.1	1120	1296	175
				5	1.87	2.20	4.0	1444	1500	55
				6	1.36	1.87	4.1	1500	1591	90
				7	0.17	0.56	4.8	1744	1825	80

*CH wear = Crown height wear / occlusal wear

3.3 Common Cycle: Chronology, and Duration of Stress and Recovery (Multiple Teeth)

3.3.1 Common Cycle (Theoretical Example)

In this paper, the use of a common cycle is proposed to objectively match defects across multiple teeth of the same individual, and from which then to estimate the chronology of defects associated with episodes of systemic stress, as well as their duration.

Figure 4 shows three identical hypothetical negative residual series, each of which has been converted to time using an equation from a different tooth type, which is used to illustrate how Solver assists in objectively creating a common cycle of defects. Series one was converted to time-based on the growth schedule of an upper central incisor, series two based on the growth schedule of an upper lateral incisor, and series three was converted using the schedule of an upper canine. As can be seen, due to the different growth schedule, the negative residual defects are all slightly out of alignment with each other.

Figure 4 Theoretical example of three Negative Residual Series with no Offset

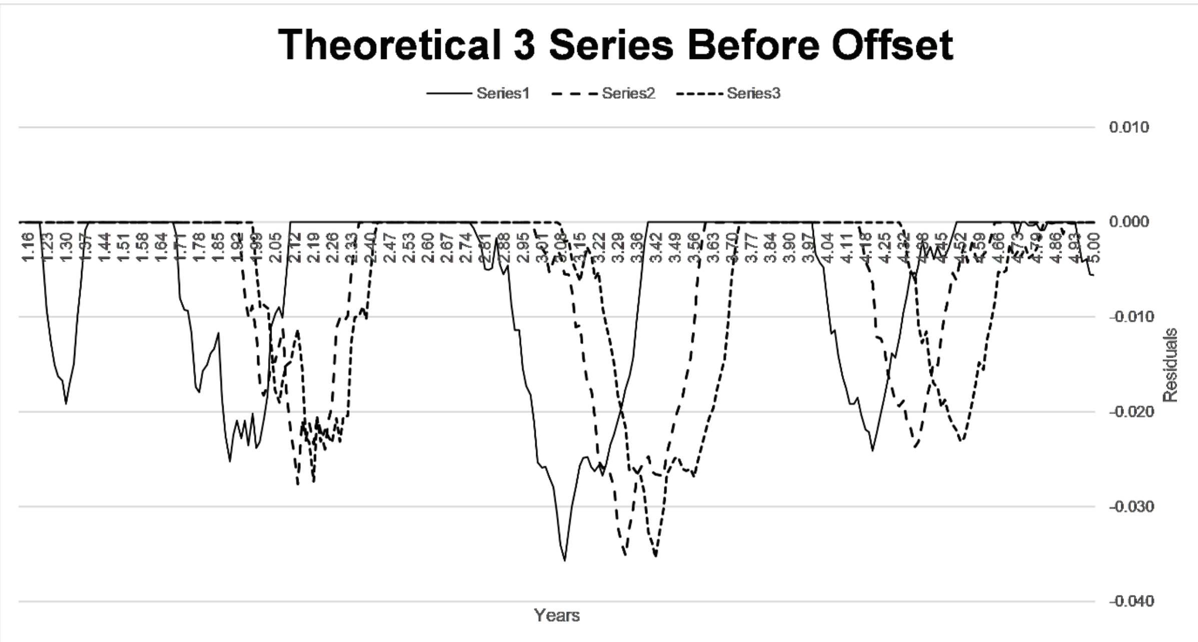

Figure 5 shows the three series after they have been offset using Solver. In this instance, Solver solved the problem (that is, finding the exact number of days that each series needed to be shifted forward or backward) to arrive at the optimum offset values for each series that would result in the highest number of instances where the data points of all three series were below one negative standard deviation. In this instance, the solution proposed was for series one to be shifted by -69.50 days, series two by -0.82, and series three by +49.91.

Figure 5 Theoretical example of three Negative Residual Series Offset using Solver

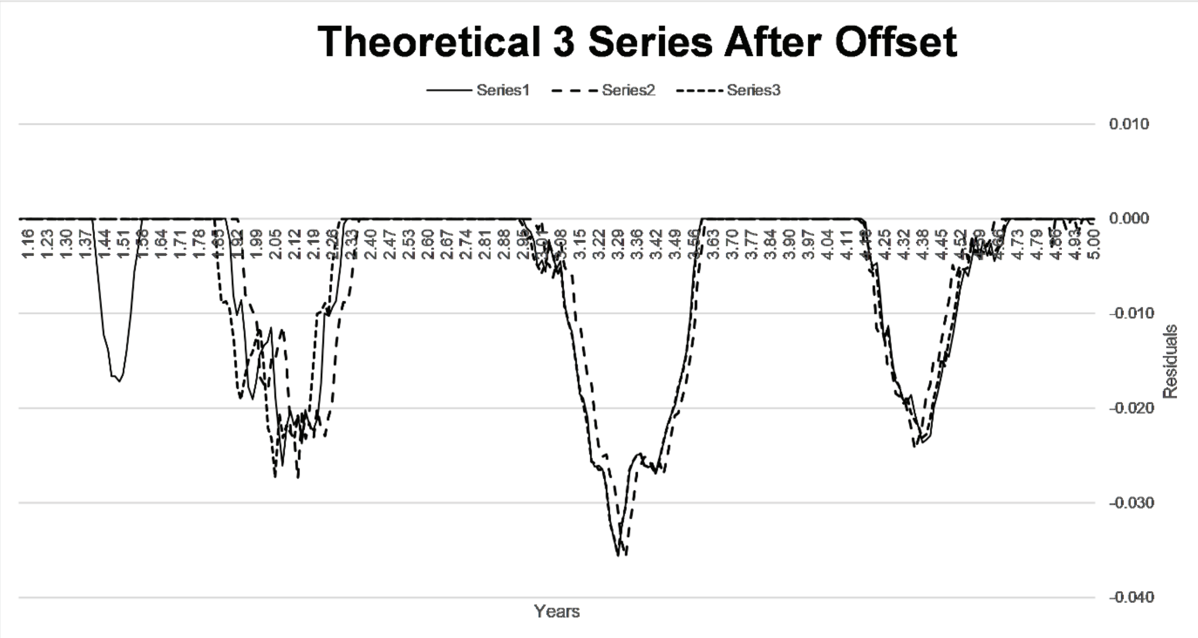

Figure 6 shows the resulting Common Cycle of defects calculated as the average of all three negative residuals series after offset.

Figure 6 Theoretical Common Cycle

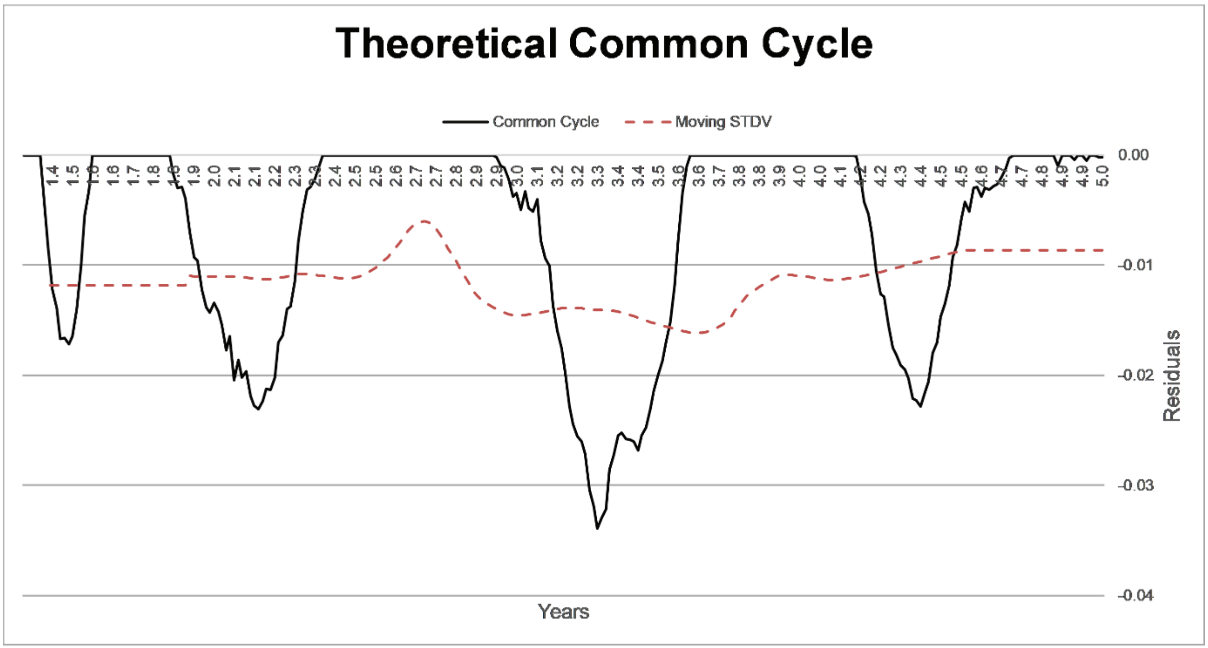

3.3.2 Common Cycles: Results for all Three Individuals

A common cycle of defects was constructed for all three individuals examined in this paper to objectively match defects representing the same episode of stress across multiple teeth of the same individual. These common cycles were then used to estimate the chronology and overall duration, as well as stress and recovery duration of the identified LEH defects. The results are presented in Table 5.

For individual 77NNM18KB, three defects were matched across the three anterior maxillary teeth examined (see Figure 7 for common cycle) and are attributable to episodes of systemic stress. The first of these (A) was identified at 2.2 years of age with a total episode duration of 180 days (6 months). The estimated stress and recovery duration were estimated to be roughly equal at 90 days each. The second LEH defect (B) was identified at 3.2 years of age, with a total episode duration of 255 days (8 and a half months). The stress duration was estimated to be approximately 135 days, with a slightly shorter recovery duration of 120 days.

The third defect (C) was identified at 4.5 years of age, with a total episode duration of 200 days (6 and a half months). Stress duration was slightly shorter, estimated at 80 days, while the recovery duration was estimated to be 120 days. The estimated total number of days of growth disruption experienced by the individual was 635 days.

Figure 7 Common Cycle of LEH defects for 77NNM18kb

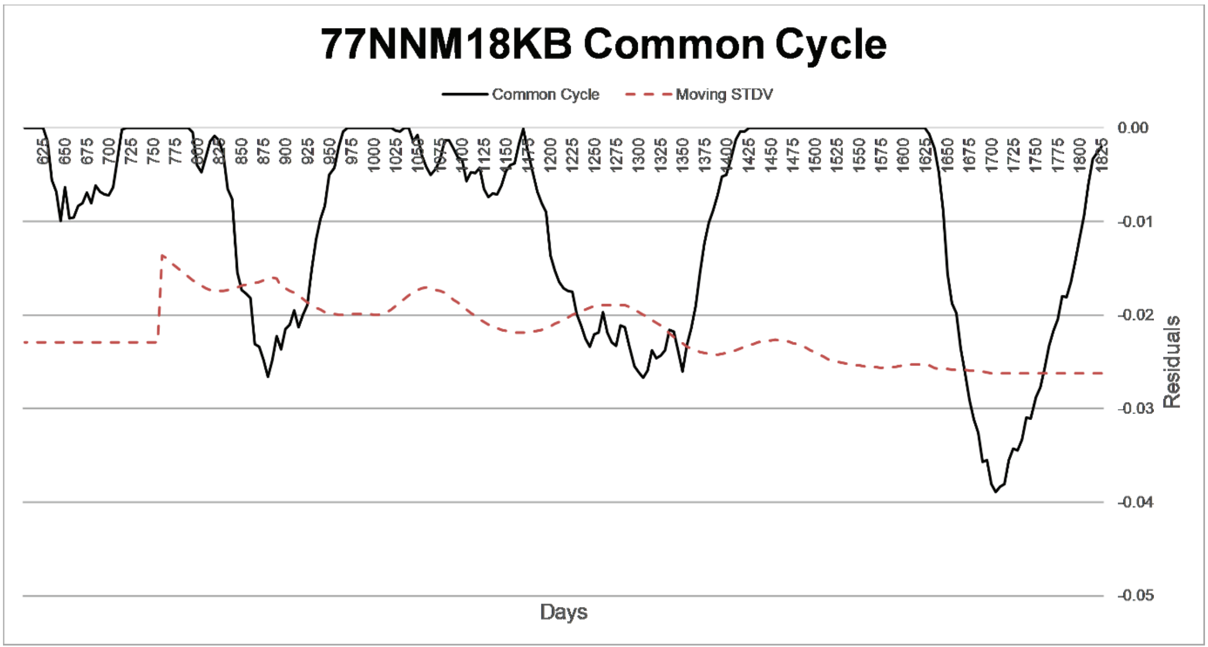

For individual 80CCNM11a, four defects were matched across the two anterior maxillary teeth examined (see Figure 8 for common cycle). However, only three of these fell below the moving standard deviation and are attributed to episodes of systemic stress. The first of these (A) was identified at 2.0 years of age, with a total episode duration of 190 days (six months). Stress duration was estimated to be 85 days, while recovery duration was slightly longer at 105 days. The second LEH defect (B) was identified at 3.1 years of age, with an overall episode duration of 135 days (four and a half months). This was comprised of an estimated 80 days of stress and a slightly shorter recovery period of 55 days. The third defect (C) was identified at 3.9 years of age, with a total episode duration of 185 days (six months). The defect was comprised of a longer stress period estimated at 130 days, with a shorter recovery of 55 days. A fourth defect (D) was identified at 4.7 years of age but was not attributed to systemic stress. Inspection of the data showed this to be an artificial defect resulting from how the polynomial fit the enamel surface near the CEJ on both the teeth that were examined. The estimated total number of days of growth disruption experienced by the individual was 510 days.

Figure 8 Common Cycle of LEH Defects for 80CCNM11a

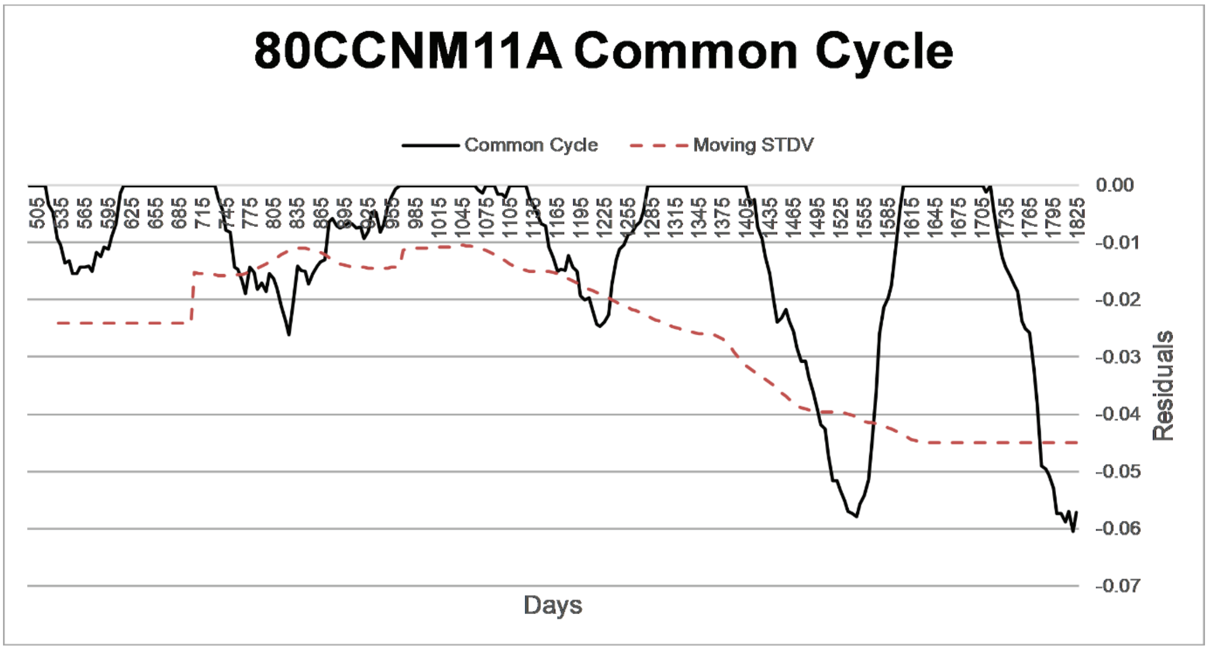

For individual 80CCNM47a, four defects were matched across the two anterior maxillary teeth examined (see Figure 9 for common cycle) and are attributed to episodes of systemic stress. The first of these (A) was identified at 1.8 years of age, with a total episode duration of 60 days (two months). Stress duration was estimated to be 45 days, while the recovery duration was estimated to have lasted considerably less time, at 15 days. The second LEH defect (B) was identified at 2.5 years of age, with the episode estimated to have lasted 125 days (four months). This episode was comprised of a stress duration estimated at 85 days, and recovery duration of 40 days. The third defect (C) was identified at 3.5 years of age, with an overall episode duration of 115 days (just under 4 months). Stress duration was estimated to be 70 days, while recovery was estimated to have lasted 45 days. The fourth defect (D) was identified at 4.1 years of age and the episode was estimated to have lasted a total of 185 days (six months). The episode was comprised of 125 days of stress duration and 60 days of recovery. The estimated total number of days of growth disruption experienced by the individual was 485 days.

Figure 9 Common Cycle of Defects for 80CCNM47a

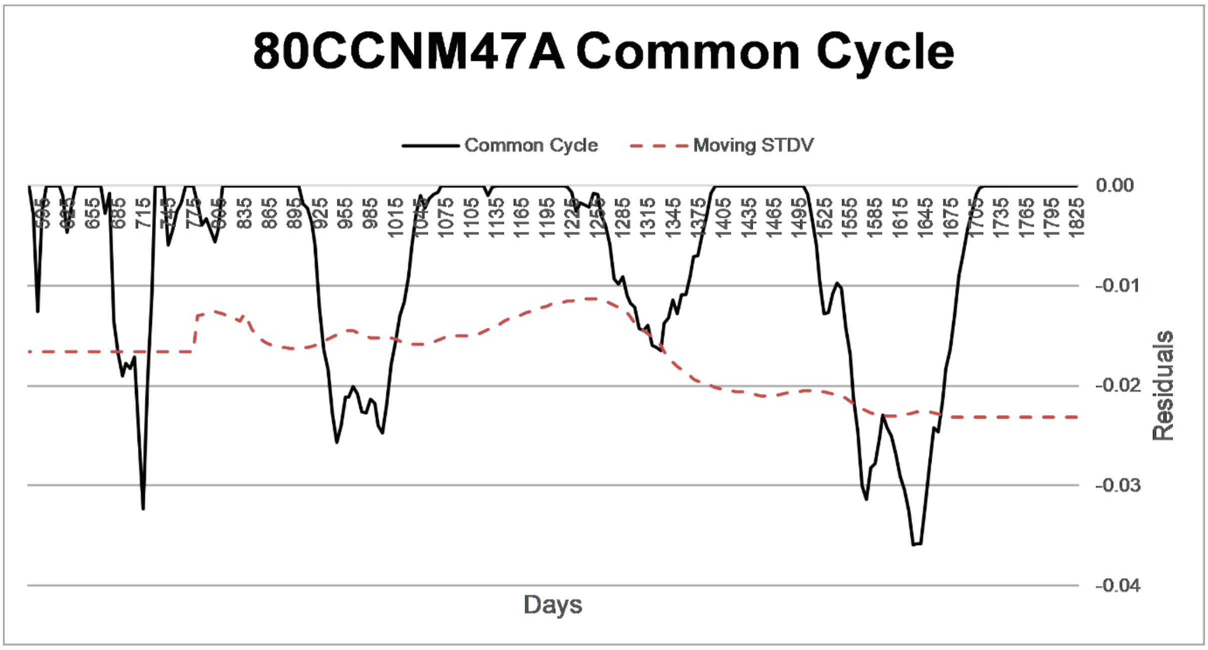

Table 5 Common Cycle of Defects Results for all Individuals

ID	Tooth	Offset	Defect	Defect Start	Defect End	Age	Recovery Start	Duration			
								Episode	Stress	Recovery	Total Disruption
77NN M18 kb	11	-184.81	A	790	970	2.2	880	180	90	90	
	22	-7.76	B	1170	1425	3.2	1305	255	135	120	635
	23	-166.98	C	1625	1825	4.5	1705	200	80	120	
80CN M11a	11	-5.4453	A	740	930	2.0	825	190	85	105	
	12	-158.23	B	1140	1275	3.1	1220	135	80	55	
			C	1415	1600	3.9	1545	185	130	55	510
			D	1720	1825	4.7	1805	105	85	20	
80CC M47a	21	-158.42	A	670	730	1.8	715	60	45	15	
	22	-96.433	B	915	1040	2.5	1000	125	85	40	
			C	1265	1380	3.5	1335	115	70	45	485
			D	1510	1695	4.1	1635	185	125	60	

4 Discussion and Conclusion

4.1 Confocal vs. Manual Custom-Built Measuring microscope

Although using laser scanning confocal microscopes such as the Sensofar or the Olympus LEXT OLS5000 can, in fact, increase the scanning time for each tooth (from approx. 15 minutes to 30-60+ minutes/tooth), much of the process is automated and therefore less labor intensive. The auto-focusing and fully automated *xy* mapping stage functionalities eliminate the need for observer judgment and consequently observer error, resulting in more accurate and precise data. Issues with manual focusing are especially problematic toward the incisal end of the tooth, where the tooth is thinner, making it more difficult to differentiate between the surface and areas just below the surface. The automated nature of the scanning process also allows the scanning of larger areas of the tooth surface in a single scan, which not only makes it easier to select the best area of the tooth surface from which to collect data (i.e. free from cracks or other obstructions) but also makes it possible to retrieve data along multiple transects on a single tooth. Although not done in this study, the recording of multiple transects may be a potential solution for eliminating noise when wanting to identify LEH using restricted sample sizes, for example when only a single tooth per individual is available for study.

That said, manual custom built measuring microscopes such as that used by Cares Henriquez and Oxenham (2017); O'Hara (2017); Temple et al. (2012), while more labor intensive, should not affect the results, and can still work equally well in terms of identifying LEH while being less expensive and requiring less time to collect surface data (approx. 10-15 minutes/tooth), albeit at a lower resolution and potentially yielding noisier data.

4.2 Artificial Defects

There are three main types of artificial defects (false positives) that can be picked up when using the method presented in this paper for identifying potential LEH defects. The first is from depressions on the tooth surface that do not extend around the crown circumference, and so cannot be considered LEH. These may be the result of pits, cracks or even from the naturally occurring labial developmental depressions if they are partially captured within a transect from the CEJ to incisal edge. This particular type of artificial defect can occur anywhere along the length of the tooth and is likely to be encountered with any method that does not rely on the presence of enamel growth lines for identifying LEH. The second type of artificial defect is from noisy data, which can be caused by inaccurate focusing, to which the incisal end of the tooth will be the most prone. This type of defect is likely to be encountered with any non-histological microscopic method but is more likely to occur when using microscopes that require observer judgment to be exercised for manual focusing. Lastly, the third type of artificial defect that might be encountered is more specifically linked to the Micro Polynomial method. These can be caused due to underfitting of the polynomial trendline and is most likely to occur at either end of the dataset (CEJ and incisal ends), as was the case with defect D on the dentition of individual 80CCNM11a. When examining individual teeth, a defect starting at distance 0.00 mm from the CEJ, is highly likely to be an artificial defect.

All three of these types of artificial defects, but in particular the first two, can be dealt with by using multiple teeth of the same individual and are likely to be canceled out during ‘matching of defects,’ which in this paper is done through the construction of a common cycle.

For the third type of artificial defect, a reduction in these false positives can be achieved by adjusting the standard deviation for the first and last 1/8 of the values, (these are areas of the tooth for which it is not possible to calculate a centred moving standard deviation due to insufficient data points), as was done in this paper (see section 2.3). However, although both the solutions mentioned above were employed, the specific curvature at the CEJ of the two teeth being examined meant that both teeth still lent themselves to underfitting when the polynomial was applied, and since both teeth were equally affected, the artificial defect was not canceled out during the construction of the common cycle. Despite this, it should be noted that this false positive was easily identifiable when looking at the charted data. Therefore, it is crucial that expert judgment be employed whenever analyzing and interpreting the results of any method that relies on quantitative data.

4.3 Matching of Defects

To minimize false positives (see section 4.2), most studies (e.g. Bennike et al. (2005); Hillson (1996); King et al. (2002); Temple et al. (2012)) recommend 'matching' of defects across multiple teeth of the same individual before they are considered to be demonstrative of LEH resulting from episodes of systemic stress. Until now, the most common method for doing this involves tabulating the particular defect ages (usually derived from a decile chart with age ranges), before the researcher decides if a defect on one tooth is deemed to be representative of another defect located at a similar chronological location on more than one tooth. Aside from being a subjective approach, this also leads to issues when a defect, based on the time range chosen to be acceptable by the researcher (usually +/- a certain number of months), might be equally representative of two different defects on another tooth. An example of this would be determining if one defect identified at 3.0 years on tooth A was more closely related to a defect at 2.8 years of age or one at 3.2 years of age on tooth B. Therefore, when examining multiple teeth, this study proposes an objective approach for identifying and constructing a common cycle of defects for the individual and then using this to estimate the average chronology and duration of stress events.

The key advantages of constructing a common cycle of defects, and following the approach as outlined in this paper are that 1) it removes the subjectivity and researcher bias, and 2) it is capable of simultaneously considering not only the specifics of each individual defect but also how the defect fits within the larger picture, that is, within the specific pattern of defects on the particular tooth and for the individual. In other words, it can quantitatively look for a pattern of defects, making it possible to see which defects are in actuality more likely to be related to another.

Furthermore, although outside the scope of this paper, theoretically, a similar approach of constructing a common cycle of defects using multiple transects of data from a single tooth for an individual could be used to identify and analyze LEH when sample sizes are restricted. In this case, the multiple transects would assist in canceling out any depressions that do not persist around the circumference of the tooth crown.

Therefore, a minimum of two teeth, with overlapping developmental schedules, is recommended to minimize false positives, with three teeth being ideal. If using a single tooth, then a minimum of three transects should be used, preferably each from a different area of the tooth, to reduce data noise.

4.4 Episode duration (Stress + Recovery)

Microscopic studies have shown that within hypoplastic defects, perikymata in the occlusal wall tend to be more widely spaced than is normal for the part of the crown in which they are located, while those in the cervical wall tend to either be normally spaced or more closely spaced than usual (Guatelli-Steinberg, 2008; Hillson, 2014; Hillson & Bond, 1997). Therefore, it is understood that stress duration is best indicated by the occlusal wall of a defect, while the cervical wall reflects a period of recovery (Hillson & Bond, 1997). Consequently, microscopic LEH studies tend only to report and consider stress duration, while disregarding recovery duration and episode duration (stress + recovery).

However, preliminary use of enamel surface depth profiles suggests that, at least externally, while there tends to be a definite general pattern of stress followed by recovery within each defect, the separation of these may not be so clear cut. Occasionally, initial recovery will be followed by a period of further decline or even equilibrium before a more pronounced and obvious recovery can be observed. This suggests that overall episode duration, as well as recovery duration, have the potential to provide valuable information about the individual experience of these periods of physiological stress, that might otherwise be unwittingly missed when focusing only on stress duration as represented by the occlusal wall of an LEH defect.

4.5 Results Comparison

Overall, there were minor differences in the number of LEH defects identified for each individual using the comprehensive approach described in this paper when compared with previous analysis using only the Micro Polynomial method by Cares Henriquez and Oxenham (2017). For individual 77NNM18KB, the previous analysis identified an additional defect at 2.8 years of age. However, using the Common Cycle approach, this was better explained as being a continuation of the defect identified at 2.2 years of age and so here was considered a single defect. For individual CCNM47a, an additional defect was identified at 1.8 years of age using the comprehensive approach presented in this paper and was attributed to systemic physiological stress. This same defect was also detected in the previous study (marked as an asterisk on Table 3 in Cares Henriquez and Oxenham (2017)) but could not be confidently associated with LEH at that time. No differences were observed for individual 80CCNM11a.

Minor differences between the two studies could also be observed in the estimated chronology of LEH episodes. This was in part due to the issues associated with relying on a decile chart to estimate the chronology of defects, especially when they fall between two decile lines. The previous study calculated the estimated age at the mid-point of the defect rather than at the start of the defect as a way to facilitate the subjective matching of defects. However, in the current study, precise and objective chronology estimates could be calculated, even when defects fell within deciles, which significantly increases the replicability of these results.

While on this occasion, the objective matching of defects using the Common Cycle approach did not substantially change the results it did, however, eliminate the potential for observer bias, while significantly increasing the replicability of the results. Finally, using the comprehensive approach presented in this paper, it was possible to calculate estimates not only for overall episode duration but also for stress and recovery periods, which was not possible in the previous study.

4.6 Recommendations

4.6.1 Reporting Standards

The reporting of both the methods used and the results of LEH analysis can vary significantly between published studies. Also, aspects relating to the use of methods which require researcher discretion (e.g., matching of defects and crown height wear estimates), are at times glossed over making it unclear as to what parameters have been used to arrive at a conclusion. This then makes it difficult for the results to be comparable with earlier or later research findings.

It is recommended, that as a minimum, the observed tooth height, as well as defect start and end locations be included when presenting the results of LEH analysis to improve both the comparability as well as replicability of results. Additionally, any crown wear estimates, as well as parameters used for estimating this, should be clearly stated. If relying on a population average for unworn crown heights, then this, as well as the number of teeth used to arrive at this value should also be included.

Furthermore, when matching of defects is undertaken, it is suggested that the precise limits employed be clearly stated. If using a common cycle approach, as presented in this paper, then this should include the Solver limits, as well as the final offset applied to each tooth. On the other hand, if using a table, then the precise +/- months difference accepted for considering two defects to be representative of the same episode of physiological stress should be stated.

4.7 Choice of methods

While subjective approaches for the recording of defects, such as the 'standard field' method put forward by Brickley and McKingley (2004) and Buikstra and Ubelaker (1994), may still prove useful as a form of preliminary analysis of samples, these should be avoided in favour of objective microscopic methods whenever possible. The latter, not only reduce observer bias and error but more importantly, yield quantitative results that have the capacity to go beyond a rudimentary discussion of LEH frequency and gradient of severity based on defect size.

LEH defects are not directly comparable to each other. This is because the width of perikymata vary, depending on where they are located on the tooth crown, decreasing in width from the incisal edge (> 100 µm) to the CEJ (<50 µm) (Hillson & Bond, 1997). Consequently, a small and narrow defect located near the CEJ region might be comprised of many perikymata and thus represent a long and or severe episode of physiological stress, while another wider and more obvious defect in the mid-crown might be comprised of only a few perikymata, and represent a shorter and milder episode of stress. Given that LEH defects are not directly comparable to each other, and with the availability of objective quantitative microscopic methods suitable even when the surface of teeth are worn and perikymata are not clearly visible, LEH frequencies are no longer an adequate way of discussing LEH. It is the details about the defect that can provide information about how the episodes of physiological stress were experienced.

4.8 Future directions

A methodological comparison using macroscopic, microscopic polynomial, and histological methods to assess LEH on a larger dataset should be undertaken to guage the extent to which results differ when using these three different approaches.

References

Bennike, P., Lewis, M. E., Schutkowski, H., & Valentin, F. (2005). Comparison of child morbidity in two contrasting medieval cemeteries from Denmark. *Am J Phys Anthropol, 128*(4), 734-746. doi:10.1002/ajpa.20233

Bocaege, E., & Hillson, S. (2016). Disturbances and noise: Defining furrow-form enamel hypoplasia. *Am J Phys Anthropol, 161*(4), 744-751. doi:10.1002/ajpa.23070

Brickley, M., & McKingley, J. (2004). Guidelines to the Standards for Recording Human Remains, IFA Paper *Institute of Field Archaeologists*. Southampton.

Buikstra, J. E., & Ubelaker, D. H. (1994). *Standards for data collection from human skeletal remains, Proceedings of a Seminar at the Field Museum of Natural History*.

Buzon, M. R. (2006). Health of the non-elites at Tombos: Nutritional and disease stress in New Kingdom Nubia. *American Journal of Physical Anthropology, 130*(1), 26-37. doi:10.1002/ajpa.20303

Cares Henriquez, A. (2019). LEH Chronology Calculator (Version 1.0). www.lehtools.com.

Cares Henriquez, A., & Oxenham, M. F. (2017). An alternative objective microscopic method for the identification of linear enamel hypoplasia (LEH) in the absence of visible perikymata. *Journal of Archaeological Science: Reports, 14*, 76-84. doi:https://doi.org/10.1016/j.jasrep.2017.05.040

Cares Henriquez, A., & Oxenham, M. F. (2018). New distance-based exponential regression method and equations for estimating the chronology of linear enamel hypoplasia (LEH) defects on the anterior dentition. *American Journal of Physical Anthropology*.

Dean, M. C., & Reid, D. J. (2001). Perikymata spacing and distribution on hominid anterior teeth. *American Journal of Physical Anthropology, 116*(3), 209.

Domett, K. M., & O'Reilly, D. J. W. (2009). Health in Pre-Angkorian Cambodia: A Bioarchaeological Analysis of the Skeletal Remains from Phum Snay. *Asian Perspectives, 48*(1), 56-78. doi:10.1353/asi.0.0016

Ensor, B. E., & Irish, J. D. (1995). Hypoplastic area method for analyzing dental enamel hypoplasia. *American Journal of Physical Anthropology, 98*(4), 507-517. doi:10.1002/ajpa.1330980410

FitzGerald, C. M. (1998). Do enamel microstructures have regular time dependency? Conclusions from the literature and a large-scale study. *Journal of Human Evolution, 35*, 371-386.

Gamble, J. A., Boldsen, J. L., & Hoppa, R. D. (2017). Stressing out in medieval Denmark: An investigation of dental enamel defects and age at death in two medieval Danish cemeteries. *International Journal of Paleopathology, 17*, 52-66. doi:10.1016/j.ijpp.2017.01.001

Goodman, A. H., & Armelagos, G. J. (1985). Factors affecting the distribution of enamel hypoplasias within the human permanent dentition. *American Journal of Physical Anthropology*.

Goodman, A. H., & Rose, J. C. (1990). Assessment of physiological perturbations from dental enamel hypoplasia and their associated histological structures. *Yearbook of Physical Anthropology, 33*, 59-110.
Goodman, A. H., & Song, R. J. (1999). Sources of variation in estimated ages at formation of linear enamel hypoplasias. In R. F. Hoppa, C. (Ed.), *Human Growth in the Past: Studies from Bones and Teeth*: Cambridge University Press.
Guatelli-Steinberg, D. (2003). Macroscopic and microscopic analyses of linear enamel hypoplasia in Plio-Pleistocene South African hominins with respect to aspects of enamel development and morphology. *American Journal of Physical Anthropology, 120*(4), 309-322. doi:10.1002/ajpa.10148
Guatelli-Steinberg, D. (2008). Using perikymata to estimate duration of growth disruption in fossil hominin teeth: issues of methodology and interpretation. In J. D. Irish, Nelson, G.C. (Ed.), *Technique and Application in Dental Anthropology* (pp. 71-86). Cambridge: Cambridge University Press.
Guatelli-Steinberg, D., Ferrell, R. J., & Spence, J. (2012). Linear enamel hypoplasia as an indicator of physiological stress in great apes: reviewing the evidence in light of enamel growth variation. *American Journal of Physical Anthropology, 148*(2), 191-204. doi:10.1002/ajpa.21619
Guatelli-Steinberg, D., Larsen, C. S., & Hutchinson, D. L. (2004). Prevalence and the duration of linear enamel hypoplasia: a comparative study of Neandertals and Inuit foragers. *Journal of Human Evolution, 47*(1-2), 65-84. doi:10.1016/j.jhevol.2004.05.004
Hassett, B. R. (2012). Evaluating sources of variation in the identification of linear hypoplastic defects of enamel: a new quantified method. *Journal of Archaeological Science, 39*(2), 560-565. doi:10.1016/j.jas.2011.10.017
Hillson, S. (1996). *Dental anthropology.* Cambridge: Cambridge University Press.
Hillson, S. (2005). *Teeth*. Cambridge: Cambridge University Press.
Hillson, S. (2014). *Tooth development in human evolution and bioarchaeology.* Cambridge: Cambridge University Press.
Hillson, S., & Bond, S. (1997). The relationship of enamel hypoplasia to the pattern of tooth crown growth: a discussion. *American Journal of Physical Anthropology, 104*, 89-103.
Hindle, A. (1998). Problems in the methodology of dental enamel hypoplasia analyses.
Hubbard, A., Guatelli-Steinberg, D., & Sciulli, P. W. (2009). Under restrictive conditions, can the widths of linear enamel hypoplasias be used as relative indicators of stress episode duration? *American Journal of Physical Anthropology, 138*(2), 177-189. doi:10.1002/ajpa.20917
King, T., Hillson, S., & Humphrey, L. T. (2002). A detailed study of enamel hypoplasia in a post-medieval adolescent of known age and sex *Archives of Oral Biology, 47*, 29-39.
King, T., Humphrey, L. T., & Hillson, S. (2005). Linear enamel hypoplasias as indicators of systemic physiological stress: evidence from two known age-at-death and sex populations from postmedieval London. *American Journal of Physical Anthropology, 128*(3), 547-559. doi:10.1002/ajpa.20232

Lukacs, J. R. (1989). Dental Paleopathology: Methods for Reconstructing Dietary Patterns. In e. M.Y. Iscan and K.AR. Kennedy (Ed.), *Reconstruction of Life from the Human Skeleton.* (pp. 261-286). New York: Alan R. Liss, Inc.

Novak, M., Vyroubal, V., Krncevic, Z., Petrinec, M., Howcroft, R., Pinhasi, R., & Slaus, M. (2018). Assessing childhood stress in early mediaeval Croatia by using multiple lines of inquiry. *Anthropologischer Anzeiger, 75*(2), 155-167. doi:10.1127/anthranz/2018/0819

O'Hara, M. (2017). Applying standard perikymata profiles to Pongo pygmaeus canines to estimate perikymata counts between linear enamel hypoplasias. *Am J Phys Anthropol, 163*(1), 213-222. doi:10.1002/ajpa.23194

Obertová, Z. (2005). Environmental stress in the Early Mediaeval Slavic population at Borovce (Slovakia). *HOMO - Journal of Comparative Human Biology, 55*(3), 283-291. doi:10.1016/j.jchb.2004.07.005

Oxenham, M. F. (2006). Biological Responses to Change in Prehistoric Viet Nam. *Asian Perspectives, 45*(2), 212-239.

Oxenham, M. F. (2016). *Bioarchaeology of Ancient Vietnam.* BAR International Series 2781: Hadrian Books.

Oxenham, M. F., Trinh, H. H., Willis, A., Jones, R. K., Domett, K., Castillo, C., . . . Piper, P. (2018). Between foraging and farming: Strategic responses to the Holocene thermal maximum in Southeast Asia. *Antiquity, 92*(364), 940-957.

Palubeckaitė, Ž., Jankauskas, R., & Boldsen, J. (2002). Enamel hypoplasia in Danish and Lithuanian Late Medieval/Early Modern samples: a possible reflection of child morbidity and mortality patterns. *International Journal of Osteoarchaeology, 12*(3), 189-201. doi:10.1002/oa.607

Pechenkina, E. A., Benfer, R. A., & Zhijun, W. (2002). Diet and health changes at the end of the Chinese neolithic: the Yangshao/Longshan transition in Shaanxi province. *American Journal of Physical Anthropology, 117*(1), 15.

Pietrusewsky, M., & Douglas, M. T. (2002). *Ban Chiang, a prehistoric village site in northeast Thailand. I, the human skeletal remains*. Philadelphia University of Pennsylvania Museum of Archaeology and Anthropology.

Reid, D. J., Beynon, A. D., Clayton, C. B., Ramirez Rozzi, F. V., Reid, D. J., & Ramirez Rozzi, F. V. (1998). Histological reconstruction of dental development in four individuals from a medieval site in Picardie, France. *Journal of Human Evolution, 35*(4–5), 463-477. doi:http://dx.doi.org/10.1006/jhev.1998.0233

Reid, D. J., & Dean, M. C. (2000). Brief communication: The timing of linear hypoplasias on human anterior teeth. *American Journal of Physical Anthropology, 113*(1), 135-139. doi:10.1002/1096-8644(200009)113:1<135::aid-ajpa13>3.0.co;2-a

Reid, D. J., & Dean, M. C. (2006). Variation in modern human enamel formation times. *Journal of Human Evolution, 50*(3), 329-346. doi:10.1016/j.jhevol.2005.09.003

Reid, D. J., & Ferrell, R. J. (2006). The relationship between number of striae of Retzius and their periodicity in imbricational enamel formation. *Journal of Human Evolution, 50*(2), 195-202. doi:10.1016/j.jhevol.2005.09.002

Sandberg, P. A., Sponheimer, M., Lee-Thorp, J., & Van Gerven, D. (2014). Intra-tooth stable isotope analysis of dentine: a step toward addressing selective mortality in the reconstruction of life history in the archaeological record. *American Journal of Physical Anthropology, 155*(2), 281-293. doi:10.1002/ajpa.22600

Shuler, K. A., Hodge, S. C., Danforth, M. E., Lynn Funkhouser, J., Stantis, C., Cook, D. N., & Zeng, P. (2012). In the shadow of Moundville: A bioarchaeological view of the transition to agriculture in the central Tombigbee valley of Alabama and Mississippi. *Journal of Anthropological Archaeology, 31*(4), 586-603. doi:10.1016/j.jaa.2012.07.001

Skinner, M. F., & Goodman, A. H. (1992). Anthropological uses of developmental defects of enamel. In S. R. K. Saunders, M. A. (Ed.), *Skeletal Biology of Past Peoples: Research Methods.* New York: Wiley.

Smith, T. M. (2008). Incremental dental development: methods and applications in hominoid evolutionary studies. *Journal of Human Evolution, 54*(2), 205-224. doi:10.1016/j.jhevol.2007.09.020

Smith, T. M., Reid, D. J., Dean, M. C., Olejniczak, A. J., Ferrrell, R. J., & Martin, L. B. (2007). New perspectives on chimpanzee and human molar crown development.

Smith, T. M., Tafforeau, P., Reid, D. J., Pouech, J., Lazzari, V., Zermeno, J. P., . . . Stringer, C., Hublin, J.J.,. (2010). Dental Evidence for Ontogenetic Differences Between Modern Humans and

Neanderthals. *Proceedings National Academy of Science, 107*, 20923-20928.

Stodder, A. L. W. (1997). Subadult stress, morbidity, and longevity in Latte period populations on Guam. *American Journal of Physical Anthropology, 104*, 636-380.

Temple, D. H. (2007). Dietary variation and stress among prehistoric Jomon foragers from Japan. *American Journal of Physical Anthropology, 133*(4), 1035-1046. doi:10.1002/ajpa.20645

Temple, D. H. (2010). Patterns of systemic stress during the agricultural transition in prehistoric Japan. *American Journal of Physical Anthropology, 142*(1), 112-124. doi:10.1002/ajpa.21208

Temple, D. H. (2014). Plasticity and constraint in response to early-life stressors among late/final jomon period foragers from Japan: Evidence for life history trade-offs from incremental microstructures of enamel. *American Journal of Physical Anthropology, 155*(4), 537-545. doi:10.1002/ajpa.22606

Temple, D. H. (2016). Chronology and periodicity of linear enamel hypoplasia among Late/Final Jomon period foragers: Evidence from incremental microstructures of enamel. *Quaternary International, 405*, 3-10. doi:http://dx.doi.org/10.1016/j.quaint.2014.12.006

Temple, D. H., Nakatsukasa, M., & McGroarty, J. N. (2012). Reconstructing patterns of systemic stress in a Jomon period subadult using incremental microstructures of enamel. *Journal of Archaeological Science, 39*(5), 1634-1641. doi:10.1016/j.jas.2011.12.021

Witzel, C., Kierdorf, U., Schultz, M., & Kierdorf, H. (2008). Insights from the inside: histological analysis of abnormal enamel microstructure associated with hypoplastic enamel defects in human teeth. *Am J Phys Anthropol, 136*(4), 400-414. doi:10.1002/ajpa.20822

*Declaration of Interest Statement

Declaration of interests

☒ The authors declare that they have no known competing financial interests or personal relationships that could have appeared to influence the work reported in this paper.